EXPERIMENTAL INVESTIGATION ON STRUCTURAL PERFORMANCE OF RC SHEAR WALLS WITH OPENINGS RETROFITTED WITH ADVANCED COMPOSITES

Ahmed Nasr[1] and Ayman S. Mosallam[2]

[1]Monifia University, Egypt
[2]♠ University of California Irvine, Irvine, USA

Abstract

Over the past few decades, retrofitting of existing buildings, rather than new construction, became more popular due to economic reasons and the benefit of shorter service interruptions of constructed facilities. Change of use of an existing building may require the removal of portions of the structural members such as introducing door and window openings in an existing shear walls. In these scenarios, a remedial retrofit of such structural members is needed to restore the structural integrity and to regain building's seismic ductility. This paper presents the results of an experimental study that aimed at evaluating the structural performance of reinforced concrete (RC) shear walls, with different opening geometries strengthened with fiber-reinforced-polymer (FRP) carbon/epoxy composites laminates. Results of this study indicated that the proposed FRP strengthening system for strengthening RC shear walls with openings was successful in significantly enhancing both the strength and ductility of the retrofitted walls. The average strength gain and ductility enhancement of the retrofitted walls, as compared to the "as-built" walls ranged from 20 % to 28%. Conclusions and recommendations for future research is presented.

Keywords: *Cyclic Shear Wall Tests, Retrofitted Reinforced Concrete shear Walls with Openings, Composites.*

♠ *Corresponding Author: mosallam@uci.edu*

1. INTRODUCTION

In recent, and due to global economic crises, retrofitting of existing buildings rather than demolishment and reconstruction has been a popular trend worldwide. The retrofit approach is considered to be environmentally friendly that reduces the amount of waste in construction. Remodeling of existing structures can sometimes include partial destruction of the structural members of a building as shear walls (i.e. introduction of windows and doors openings, ducts and stairwells, etc.). In these cases, load-bearing walls with added openings must be strengthened to accommodate for the loss of strength and ductility resulting from such alteration. Conventional retrofit techniques include epoxy injection, concrete and steel plating. In the past two decades or so, polymer composites was introduced as an attractive strengthening alternative in different applications (Mosallam et al. 2014). Some of the successful application of composites include external strengthening of existing structures constructed from different conventional materials such as steel (e.g. Mosallam, 2007[a]), reinforced concrete (e.g. Mosallam, 2000, Haroun et al., 2003, Mosallam et al., 2012, Kim et al., 2013, Mosallam et al. 2015), masonry (e.g. Mosallam, 2007[b], Mosallam and Banerjee, 2011), and wood (e.g. Mosallam et al., 2014).

The majority of published research related to reinforced concrete wall strengthening, focused on solid RC shear walls (e.g. Lombard et al., 2000, Hiotakis, 2004, Khalil and Ghobarah 2005, Antoniades et al. 2007, Meftah et al., 2007, Dan, 2012, Li and Lim, 2010, El-Sokkary et al. 2013 and Zhou et al. 2013). There are very limited studies that evaluated the behavior of RC walls with opening strengthened with polymer composites (e.g. Paterson and Mitchell, 2003, Choi et al., 2012, Mohammed et al., 2013 and Popescu et al., 2015). Paterson and Mitchell (2003) tested four RC shear walls with non-ductile reinforcement details under reversed cyclic loading. Three different retrofit schemes were evaluated namely; (i) steel headed reinforcement, (ii)

carbon/epoxy composites, and (iii) reinforced concrete collars at the base of the wall. Results of the study indicated that the combined use of headed reinforcement and carbon/epoxy composite laminates resulted in both increasing the confinement of walls' boundary element regions and the anchorage of the transverse reinforcement. In 2013, Choi et al. reported results of a study focused on structural behavior of reinforced concrete walls with opening retrofitted with carbon/epoxy laminates, and steel plates and wires. In their investigation, five shear wall specimens were tested under sustained axial load and fully revered cyclic lateral loads. Test results showed that the ultimate failure modes of the retrofitted walls were influenced by the retrofit type. Mohammed et al. (2013) presented the results of an experimental study focused on the structural performance of carbon/epoxy-strengthened RC walls panels with openings. The results of the study indicated that walls where CFRP composite laminates were applied at a 45^{o} at the opening corners had a better behavior as compared to walls where the composite plies were applied along the opening perimeters. Popescu et al. (2015) conducted a review on RC walls weakened by openings as compression members. In this paper, several design aspects were discussed that included the size and openings positions and the roles of boundary conditions and geometric characteristics on the overall behavior of such walls. In addition, the behavior of performance FRP-strengthened walls was presented.

In this paper, five large-scale reinforced concrete shear walls were experimentally evaluated under a combined sustained axial compression/cyclic lateral loading conditions. The purpose of the testing program was to evaluate the effectiveness of a new FRP retrofit details in restoring the loss of capacity due to the introduction to different openings. The results indicated that the proposed external strengthening system evaluated in this study succeeded not only in restoring

the original capacity of the solid walls (prior to introduction of openings), but in some cases, the strength of the retrofitted walls were higher than the as-built solid shear wall.

2. EXPERIMENTAL PROGRAM

2.1 General: In this study, five large-scale reinforced concrete shear wall specimens were tested. Each wall specimen consisted of a wall base 2,438 mm (8 ft) X 914 mm (3 ft) X 609 mm (2 ft), a wall panel with same dimensions of 1.828 m (6 ft) X 1.828 m (6 ft) X 203 mm (8 inches) [*Width X Length X Thickness*] and a load-transfer RC cap beam with dimensions of 2.133 m (7 ft) X 609 mm (2 ft) X 609 mm (2 ft) [*Length X Width X Depth*] as shown in Figure (1). Each wall specimen had two RC boundary elements reinforced with 4#4 (4ϕ12.7 mm) steel rebars each. The wall was internally reinforced with 4#3 (4 ϕ 9.5 mm) steel rebars spaced at 305 mm (12 inches) on center and 6#3 (10 mm) spaced at 305 mm (12 inches) on center at each face (refer to Figure 1). The first specimen, designated herein as (C-S), is a solid RC shear wall without any openings. This specimen was used as a control "as-built" specimen to determine its capacity as compared to walls with openings. The second specimen (C-WO) has 604 mm (2 ft) X 609 mm (2 ft) window opening at the center of the wall and the third specimen (C-DO) has 457 mm (1.5 ft) by 1,219 mm (4 ft) door opening near the edge of the wall (see Figure 1). Both the second and the third walls were used as control specimens to determine the loss in capacity after different openings were introduced. The forth specimen (R-WO) has the same opening configuration as the second wall specimen (C-WO) and the fifth specimen (R-DO) had opening configuration as the third wall (C-DO), however, these later three walls were strengthened with CFRP wet layup composite laminates. Table (1) presents a summary and description of different walls evaluated in this study. Typical dimensions, reinforcement details and opening geometry of wall specimens are shown in Figure (1).

2.2 Wall Specimens Fabrication: The five wall specimens evaluated in this study were casted together on the same day using same concrete patch. Concrete cylinders were tested at 28 days as well as on the day of each test. Table (2) shows test results for concrete cylinders compressive strength. As mentioned earlier, # 3 (9.50 mm) and #4 (12.70 mm) deformed steel rebars were used for all walls vertical reinforcement, while #3 (9.50 mm) rebars were used as walls' horizontal reinforcement. All steel reinforcing rebars were Grade 60-A615. The experimental mechanical properties of the reinforcement steel used in reinforcing the wall specimens are presented in Table (3). In this study, one type of FRP system was used; namely carbon/epoxy wet lay-up unidirectional composite laminates. Table (4) presents the mechanical properties obtained from ASTM D-3039 coupon tests using single-ply and 2-ply coupons.

2.3 Shear Walls Test Setup: The typical test set-up of the tested wall specimens is shown in Figure (2). A calibrated 400-kip (1,780-kN) servo-hydraulic actuator was used to apply the lateral cyclic loads to all specimens according to a defined loading protocol. A steel cross beam, two hydraulic jacks, steel threaded rods connected to the laboratory strong floor with steel hinges were used to allow horizontal movement of the wall cap while maintaining a constant value for the applied axial compression load. In order to simulate typical earthquake loading for these large-scale tests, an in-plane full-reversal cyclic loading protocol described by the International Code Council (ICC) Evaluation Service (ES)'s *Acceptance Criteria for Concrete and Reinforced and Unreinforced Masonry Strengthening Using Fiber-Reinforced Polymer (FRP), Composite Systems* (ICC-ES AC125-10, 2010) was adopted for all tests (refer to Figure 3). Prior to applying the full-reversal lateral cyclic loads, an axial compression load of 10% of the wall's 28-day compressive strength (1,034.6 kN/230 kips) was applied on the wall top simulating the gravity load wall. Lateral displacements at different locations along the wall height were measured using string potentiometers (String Pots). The locations of the string pots are as illustrated in Figure (4).

2.4 Application of FRP Composites: All retrofitted wall specimens were strengthened using the following procedure. Prior to installing the FRP composite laminates, concrete surface was grinded to smooth out irregularities and the sharp edges were rounded to a radius of about 25.4 mm (1″). After grinding, surface voids were patched using epoxy putty. Preior to the installation of the composite laminates, a thin coat of low-viscosity epoxy primer was applied to the surface. The impregnated composite laminate was applied at the marked positions in accordance to the designed retrofit scheme. Composite laminates were pressed to squeeze any excess resin and air bubbles and were secured in place by pressing using a harder roller. It was ensured to remove entrapped air under the laminates to achieve good bond between the laminates the concrete substrate.

As stated earlier, both wall specimen (R-WO) and (R-DO) were retrofitted in both flexure and shear. Due to the existence of direct connection between the left and right piers and the wall footing, a special anchorage system was installed for wall specimen (R-DO) to ensure the transfer of forces between the wall base and the vertical FRP laminates. The anchorage system consisted of steel angles and high-strength steel threaded rods. Figure (5) shows the details of the retrofit systems for both retrofitted walls (R-WO) and (R-DO) and the anchorage system for wall specimen (R-DO).

3. Experimental Results

The following paragraphs describe both details and results of the large-scale tests conducted on the five shear wall specimens.

3.1. Control Solid Wall (C-S): The objective of this test is to evaluate the performance of the as-built solid wall (prior to introduction of openings) that is used later for comparison with

behavior of wall specimens with openings. The wall was designed and detailed according to *Building Code Requirements for Structural Concrete and Commentary* (ACI318-11). Control solid wall specimen (C-S) was tested up to failure to determine the ultimate load capacity, cracking pattern and hysteric response under combined axial compression/lateral cyclic loading. In all tests, a lateral load-control protocol was applied with the following steps: ±133.45kN (±30 kips), ±266.90kN (±60 kips), ±400.4 kN (±90 kips), ±444.80 kN (±100 kips), ±489.30kN (±110 kips), ±533.80kN (±120 kips), ±578.27kN (±130 kips), up to the point where first yield of the vertical rebars is detected. Initial cracks were observed at a load level of 400.40 kN (90.0 kips) during the push-cycle at both sides of the wall at different locations. During the push-cycle, the first yield of the reinforcement steel was detected at a load level of 533.8 kN (120 kips) that occurred at the bottom of the wall corresponding. At this first yield load, the corresponding displacement was 6.35 mm (¼″). After the occurrence of the first yield, and according to the ICC-ES AC15 requirements (refer to Figure 3), the load-controlled loading was changed to a displacement-control protocol with the following steps: ±6.35mm (±0.25″), ±9.53mm (± 0.375″), ±12.70mm (±0.50″), ±19.0mm (±0.75″), ±25.40mm (±1.00″), and ±38.10mm (±1.50″). These displacement steps correspond to ductility indices (of 1.00, 1.50, 2.00, 3.00, 4.00 and 6.00, respectively. The ductility index used in calculating the preceding ductility values is defined as:

$$\mu_d = \frac{\Delta_d}{\Delta_y} \tag{1}$$

where Δ_d is the demand displacement and Δ_y is the idealized yield displacement.

As the lateral load increased, a local crushing damage at the wall's toe was observed due to excessive compressive stress. The toe crushing was first occurred at the compression side of the wall during the push-cycle associated with a lateral displacement of 31.80 mm (1.25″) that corresponds to a lateral load of 765.1 kN (172 kips). Loading continued beyond this event to

observe the ultimate wall behavior and to identify the ultimate failure mode of the wall specimen. The maximum load in the pull-direction was 831.8 kN (187 kips) that corresponds to a lateral displacement of 38.00 mm (1.50″). During the second cycle of ductility 6.00, diagonal cracks were developed leading to a diagonal shear ultimate failure of the wall as shown in Figure (7). The load-displacement hysteretic curve for this wall specimen is shown in Figure (8).

3.2 Unstrengthened Control Wall with Window Opening (C-WO): The purpose of this test is to evaluate the behavior of unstrengthened shear wall when a central window opening (C-WO) that was not included in the original design (refer to Figure 1). As for the previous test, a constant axial compression load was applied to the wall top. Few hair cracks were observed at the cap beams as the compression axial load was applied. Upon the application of the lateral load, no cracks were visually detected up to a load level of 266.90 kN (60.00 kips). Beyond this lateral load, the length of the initial crack that was initiated during axial compression load application slightly increased. The first-yield of the reinforcement steel was detected at a load level of 489.30 kN (110.00 kips) in push cycle at the bottom of the wall at the most extreme rebar layer corresponding to a displacement of 5.1 mm (0.20″). A displacement-control protocol with the following steps ±5.10mm (±0.20″), ±7.60 mm (±0.30″), ±10.16mm (±0.40″), ±15.24mm (±0.60″), ±20.32mm (±0.80″), and ±25.40mm (±1.0″). These displacement steps correspond to ductility indices (μ_d) of: 1.00, 1.50, 2.00, 3.00, 4.00 and 5.00, respectively. The first local damage occurred at the wall's left pier in the form of a diagonal shear failure. This local damage occurred at a displacement of 19.00 mm (0.75″) that corresponds to a load level of 680.6 kN (153 kips). The maximum load resisted by this wall specimen in the pull direction was 725.1 kN (163 kips) that corresponds to a lateral displacement of 20.30mm (0.80″). During the pull- cycle of a lateral displacement of 25.4 mm (1.00″), the wall's right pier failed in diagonal shear. Figure (9) shows

the ultimate failure mode of this wall specimen. The load-displacement hysteretic curve is presented in Figure (10).

3.2. Control Wall with Door Opening (C-DO): The objective of testing this wall specimen was to assess the effect of introducing a relatively large opening as compared to the area of the original as-built solid on structural behavior of the wall. As for the previous tests, initially, a load-control protocol was used with the following load steps: ±133.45kN (±30.00 kips), ±266.90kN (±60.00 kips), ±400.34kN (±90.00 kips), ±444.80kN (±100.00 kips), ±489.30kN (±110.00 kips), ±533.80kN (±120.00 kips), ±578.27kN (±130.00 kips), ±622.75kN (±140 kips) until the first yield occurred. The first yield of the vertical reinforcing steel was detected at a load level of 444.8 kN (100.00 kips) during the push-cycle at the top right-hand corner of the wall opening. The corresponding displacement at the yield load was about 5.10 mm (0.20″). After reaching the first yield, the load-control loading protocol was replaced by a displacement-control protocol with the following steps: ±5.08mm (± 0.20″), ±7.62mm (± 0.30″), ±10.16mm (± 0.40″), ±15.24 (± 0.60″), ±20.32mm (± 0.80″) and 25.40mm (± 1.00″). The corresponding ductility indices (μ_d) were calculated using Eq. (1) as: 1.00, 1.50, 2.00, 3.00, 4.00 and 5.00, respectively. At a displacement of 9.10 mm (0.36″) during the pull-cycle, a diagonal crack was observed at the top right-hand corner of the door opening. As the applied lateral displacement increased, and at about a displacement of 20.30 mm (0.80″), several diagonal cracks were formed at both wall pier in both pull- and push- cycles of this lateral displacement level. The maximum load resisted by this wall specimen in the push direction was 711.70 kN (160.00 kips) that occurred at a displacement level of 20.30mm (0.80″). At the push-cycle of displacement level of 24.10 mm (0.95″), diagonal cracks at the left pier propagated and connected together leading to a diagonal shear failure of the left pier. The maximum load in the pull direction was 725.10 kN (163.00 kips) that corresponds

to a lateral displacement of 22.90 mm (0.90″). The second local damage occurred at the right narrow pier at lateral displacement level of 24.10 mm (0.95″) during the pull direction. This damage was in the form of concrete crushing of both the top left and bottom right corners of the pier as shown in Figure (11). The load-displacement and load-drift ratio hysteresis curves for this unstrengthened wall specimen are shown in Figures (12).

3.3. ***Retrofitted Wall with Window Opening (R-WO):*** This wall specimen was tested under both sustained compressive vertical load and full-reversal lateral cyclic loads up to failure. The objective of conducting this test was to evaluate the effectiveness of the proposed FRP composite retrofit scheme in upgrade in restoring the wall strength and ductility. Identical cyclic loading history as per Figure (3) was applied, initially, as a force-control mode, that was followed to a displacement-control mode when reaching the first yield as for the previous tests. The load-control protocol was applied using following load steps: ±133.45kN (±30.00 kips), ±266.90kN (±60.00 kips), ±400.34kN (±90.00 kips), ±444.80kN (±100.00 kips), ±489.30kN (±110.00 kips), ±533.80kN (±120.00 kips), ±578.27kN (±130.00 kips), ±622.75kN (±140 kips) until the first yield occurred. No cracks were detected in the wall till the first yield of the vertical reinforcement. The first yield of the vertical reinforcement steel was observed at a load level of 120 kips (533.8 kN) in the pull and push direction at the same time and the corresponding displacement was 0.25 inches (6.30 mm). The displacement-control loading protocol with the following steps: ± 6.30 mm (± 0.25″), ± 9.52mm (± 0.375″), ± 12.70mm (± 0.50″), ± 19.05mm (± 0.75″), ± 25.40mm (± 1.0″), ±31.75mm (± 1.25″), and ± 38.10mm (± 1.50″). The corresponding ductility indices (μ_d) were calculated using Eq. (1) as: 1.00, 1.50, 2.00, 3.00, 4.00, 5.00 and 6.00, respectively.

At a ductility level 1.50 (corresponds to a lateral displacement of 9.5 mm/0.375″) during both the pull- and push- cycles, two cracks were observed at the two top corners of the window opening, however, no damage to the CFRP laminates was observed. During the first cycle of ductility level 3.0 (corresponds to a lateral displacement of 19.00 mm/0.75″), a minor deboning started to occur at the horizontal CFRP laminates located at bottom of the window opening at both sides of the wall. A partial debonding of the horizontal U-shaped CFRP composite laminates located between the bottom spandrel and both left and right wall piers. No additional cracks were observed up to the ultimate failure of this wall specimen, however, debonding of the bottom CFRP U-shaped laminates at both the left and right wall piers continued to grow. Loading continued beyond this point in order to determine the wall's ultimate load. The maximum load in the push-direction was 956.40 kN (215.00 kips) that occurred at a lateral displacement of 31.80mm (1.25″), while the maximum load in the pull-direction was 898.60 kN (202.00 kips) that occurred at a lateral displacement of 31.80mm (1.25″). At a displacement level of 38.10mm (1.50″) and during both the pull- the push-cycles, fracture at the edges of the horizontal laminates at both the top and bottom of the opening was noticeable. At the same time, the horizontal CFRP U-shaped laminates at the bottom of the wall piers suffered from severe debonding and started to dilate resulting in concrete crushing as shown in Figure (13). The load-displacement and load-drift ratio hysteresis curves are shown in Figure (14).

3.4. Retrofitted Wall with Door Opening (R-DO)

Wall Specimen (R-DO) was retrofitted with carbon/epoxy composite laminates following the retrofit scheme shown in Figure (5-b). After the retrofit system is applied and cured, the wall specimen was tested under vertical loading and lateral cyclic loading up to failure to assess the proposed retrofit schedule and evaluate the behavior of the wall specimen. A load control

protocol similar to the one sued for wall specimen (R-WO) was applied until yield is detected. After the yield was detected, the displacement control protocol with the following steps ± 0.30″, ± 0.60″, ± 0.90″, ± 1.20″, ± 1.50″ equivalent to ductility level of 1.00, 2.00, 3.00, 4.00, 5.00, respectively was applied to the specimen up to failure. At the third cycle of ductility level 2.0 of displacement 15.20mm (0.60″) partial debonding of vertical CFRP laminates on right narrow pier at wall top at 15.20mm (0.60″). At the first cycle of ductility level 3.0 of displacement 22.90 mm (0.90″) another crack occurred at the top of the opening and at the same time debonding of vertical CFRP laminates on wide left pier next to the opening has initiated at wall top. In The first cycle of ductility level 4.0 of displacement 31.80mm (1.20″) the debonding of vertical CFRP laminates on right narrow pier at wall top began to grow up to a displacement 25.40 mm (1.00″) resulting in severe splitting of the concrete cover exposing the wall rebars and resulting in significant drop in the wall load capacity. The test was stopped at this point and the wall specimen at the end of the test is shown in Figure (14). The maximum load in the push was 1,005.30 kN (226.00 kips) at displacement of 22.90mm (0.90″) and the maximum load in the pull was 791.80 kN (178.00 kips) at displacement of 22.90 mm (0.90″). Figure (15) shows the load-displacement hysteretic curve for shear wall specimen (R-DO).

3.5. Comparisons of the Results of Different Wall Specimens

In order to evaluate the improvement in seismic performance of the retrofitted specimen, the modes of failure of both the control and retrofitted specimen were identified based on the observation of test results. The mode of failure and ductility are the main goals for measuring the improvement of seismic performance of the control walls with openings when retrofitted with the proposed retrofitting systems and schemes. For the control solid wall, the observed mode of failure was concrete crushing at the wall toe after experiencing a lot of flexure cracks and diagonal

shear cracks followed by diagonal shear failure of the wall due to excessive displacement. For the control wall with window opening (C-WO), the behavior of the wall was ductile up to failure but the mode of failure was different the left and right piers of the wall failed at the end of the test in diagonal shear rather than flexure failure by concrete crushing. Control wall with door (C-DO) had different modes of failure in each pier. The left wide pier experienced shear failure while the right narrow pier had diagonal shear cracking but at the end of the test failed in flexure by crushing of concrete at the top and bottom sections. For the retrofitted specimen, retrofitted wall with window (R-WO) and retrofitted wall with door (R-DO) no shear failure occurred. The failure sequence for both specimens was the debonding of the CFRP laminates from the concrete surface specially the vertical inner laminates on the side of the opening at the top of the wall and then towards the end of the test flexure failure at the zone between spandrels and the wall piers. A comparison of the failure mode for all the specimens is presented in Table (5). The load-displacement envelopes for all specimens are compared in Figure (16). Figure (17) shows at comparison of the average load capacities of all tested walls. It can be seen from the graphs that the retrofitted specimens had higher capacities than the solid control wall (C-S). Comparison between the different ductility levels achieved by different specimens up to failure is shown in Table (6).

4. CONCLUSIONS

Results of the current study indicated that the proposed FRP composites systems evaluated in this study for strengthening RC shear walls with openings was successful in enhancing the overall performance of the retrofitted walls over the control walls with openings and control solid wall too. As expected, the structural capacity of RC walls with openings was lower than those without openings (solid walls). The peak loads of the control wall with window opening and the control

wall with door opening were about 13% less than that of the control solid wall (C-S) with the introduction of the openings that were not included in the original solid wall design. The proposed carbon/epoxy (CFRP) external strengthening system designed in this study for retrofitting RC shear walls with openings achieved significant increase in the strength of the retrofitted walls as compared to the control walls with openings. The average peak load of the retrofitted wall with window opening (R-WO) was 1.32 times the average peak load of the control wall with window opening (C-WO). For the retrofitted wall with door opening (R-DO), the average peak load was 1.25 times the average peak load of the control wall with door opening (C-DO). This study confirmed the impact of the opening geometry, size and location on the ductility characteristics of RC walls. For example, results obtained from the large-scale experimental program indicated that the ductility index of the RC shear wall with window opening (R-WO) retrofitted with carbon/epoxy laminates has increased to 6 as compared to a ductility index of 5 for the control RC shear wall specimen with window opening (C-WO). It was also shown that the effectiveness of the retrofit system on enhancing the wall ductility is also dependent on the geometry, size and location of the opening. For instant, the ductility of the retrofitted wall with door opening (R-DO) was 3.33 compared to 5 for the control wall with door opening (C-DO) due to the localized severe debonding failure of the retrofitted wall at the connection between the top spandrel and the narrow wall pier. The anchorage system developed in this study for wall (R-DO) to transfer the forces generated in the vertical CFRP laminates at the wall base had a satisfactory performance. As evidence to this conclusion, there was no sign of debonding or visual local damages between the steel angle or the CFRP laminates and no damage to the steel angle or the threaded rods up to the ultimate load. In this study, no anchors were used where the FRP laminates were terminated. It should be noted that in this study, no anchors were used where the FRP laminates were

terminated. The performance of the retrofit systems could have been greatly improved if anchoring systems were provided at the locations where laminates end.

REFERENCES

ACI Committee 318 (2011), Building Code Requirements for Structural Concrete and Commentary (ACI 318-11), American Concrete Institute, Detroit, MI, 430 pp.

ACI Committee 440. Guide for the Design and Construction of Externally Bonded FRP Systems for Strengthening Concrete Structures, ACI 440.2R-08, Farmington Hills, MI; 2008.

ASTM D3039/D3039M − 14 (2014). Standard Test Method for Tensile Properties of Polymer Matrix Composite Materials, ASTM International, West Conshohocken, PA, USA.

Antoniades, K.K., Salonikios, T.N., and Kappos A.J. (2003). "Cyclic Tests On Seismically Damaged Reinforced Concrete Walls Strengthened Using Fiber-Reinforced Polymer Reinforcement". ACI Struct. J., 100(4), pp. 510-518.

Antoniades, K.K., Salonikios, T.N., and Kappos, A.J. (2005). "Tests on Seismically Damaged Reinforced Concrete Walls Repaired and Strengthened Using Fiber-Reinforced Polymers", Journal of Composites for Construction, ASCE, 9(3), 236-246.

Antoniades, K.K., Salonikios, T.N., and Kappos, A.J., (2007). "Evaluation Of Hysteretic Response and Strength of Repaired R/C Walls Strengthened With FRP". Engineering Structures 29, pp. 2158-2171.

Choi, Y-C., Choi, H-K, Lee, M-S and C-S Choi (2012). "A study on the retrofit method of a shear wall by new openings". Magazine of Concrete Research, Volume 64, Issue 5, p.p. 377 –39, DOI: 10.1680/macr.10.00112.

Dan, D. (2012). "Experimental tests on seismically damaged composite steel concrete walls retrofitted with CFRP composites," Engineering Structures, Volume 45, December, p.p. 338–348

El-Sokkary, H., Galal, K., Ghorbanirenani, I., Léger, P., and Tremblay, R. (2013). "Shake Table Tests on FRP-Rehabilitated RC Shear Walls." ASCE J. Compos. Constr., 17(1), p.p. 79–90.

Zhou, H, Attard, T.L., Zhao, B., Yu, J., Lu, W. and L. Tong (2013). "Experimental study of retrofitted reinforced concrete shear wall and concrete-encased steel girders using a new CarbonFlex composite for damage stabilization," Engineering Failure Analysis, Volume 35, December, p.p. 219–233.

Hiotakis, S., (2004). "Repair and Strengthening of Reinforced Concrete Shear Walls for Earthquake Resistance Using Externally Bonded Carbon Fibre Sheets and a Novel Anchor System" Master Thesis, Carleton University.

ICC-ES, AC125 (2010). Interim criteria for concrete and reinforced and unreinforced masonry strengthening using fiber-reinforced polymer (FRP) composite system, ICC-Evaluation Service Inc.

Khalil, A. and Ghobarah, A., (2005) "Behaviour of Rehabilitated Structural Walls" Journal of Earthquake Engineering, 9(3), 371-39.

Kim, J. J., Noh, H.-C. A., Taha, M. M., Mosallam, A. S. (2013). "Design Limits for RC Slabs Strengthened with Hybrid FRP–HPC Retrofit System," Composites Part B: Engineering, 51, pp. 19–27.

Li, B. and Lim, C. (2010). "Tests on Seismically Damaged Reinforced Concrete Structural Walls Repaired Using Fiber-Reinforced Polymers." ASCE J. Compos. Constr., 14(5), 597–608.

Lombard J. C. (1999), "Seismic Strengthening and Repair of Reinforced Concrete Shear Walls Using Externally Bonded Carbon Fiber Tow Sheets", Master of Engineering Thesis, Carleton University, Ottawa, Ontario, Canada.

Lombard J., Lau D. T., Humar J. L., Foo S., Cheung M. S. (2000) " Seismic strengthening and repair of reinforced concrete shear walls" Proc., Twelfth World Conf. on Earthquake Engineering, (CD-ROM), New Zealand Society for Earthquake Engineering, Silverstream, New Zealand, Paper No. 2032.

Meftah, S.A., Yeghnem, R., Tounsi A., and. Adda bedia, E.A, (2007) "Seismic Behavior of RC Coupled Shear Walls Repaired with CFRP Laminates Having Variable Fibers Spacing", *J. Construction and Building Materials* 21 (8), pp. 1661–1671.

Mosallam A. S. (2000). "Strength and Ductility of Reinforced Concrete Moment Frame Connections Strengthened with Quasi-isotropic Laminates," Composites Part B: Engineering, Vol. 31B, No. 6/7, pp. 481-497.

Mosallam, A.S. (2007). "Structural Evaluation and Construction of FRP Composites Strengthening Systems for the Sauvie Island Bridge," Composites in Construction Journal, American Society of Civil Engineers (ASCE), Volume 11, Issue 2, March/April, pp. 236-249.

Mosallam, A.S. (2007). "Out-of-Plane Flexural Behavior of Unreinforced Red Brick Walls Strengthened with FRP Composites," Composites Part B: Engineering, Volume 38, Issues 5-6, July-September, pp. 559-574.

Mosallam, A. S., and S. Banerjee, (2007). "Shear Enhancement of Reinforced Concrete Beams Strengthened with FRP Composite Laminates". Composites B: Engineering, 38 (5–6), pp. 781–793.

Mosallam, A.S. and S. Banerjee (2011). "Enhancement in in-plane shear capacity of unreinforced masonry (URM) walls strengthened with fiber reinforced polymer composites," Composites Part B: Engineering Volume 42, Issue 6, September, pp. 1657-1670.

Mosallam, A.S., Taha, M.M., Kim, J.J., and A. Nasr (2012). "Strength and ductility of RC slabs strengthened with hybrid high-performance composite retrofit system," Engineering Structures, Volume 36, March 2012, pp. 70-80.

Mosallam, A.S., Bayraktar, A., Elmikawi, M., Pul, S. and S. Adanur (2014). "Polymer Composites in Construction: An Overview," SOJ Materials Science & Engineering, Vol. 2, Issue 1, pp. 1-25.

Mosallam el al. (2015). "Structural Evaluation of Reinforced Concrete Beams Strengthened with an Innovative Bolted/Bonded FRP Composites Sandwich Panels", Composite Structures Journal, Vol. 124, pp. 421–440, http://dx.doi.org/10.1016/j.compstruct.2015.01.020.

Nasr, A. (2011). Seismic Performance of RC Shear Walls with Openings Strengthened Using Advanced Composites, Ph.D. Dissertation, University of California, Irvine, California, USA.

Paterson, J. and Mitchell, D. (2003). "Seismic Retrofit of Shear Walls with Headed Bars and Carbon Fiber Wrap." J. Struct. Eng., 129(5), 606–614.

Popescu, C., Sas, G., Blanksvärd, T., and B. Täljsten (2015). "Concrete walls weakened by openings as compression members: A review," Engineering Structures, Volume 89, April, p.p. 172–190

List of Tables

Table (1): Shear Walls Test Matrix

Table (2): Concrete Compressive Strength

Table (3): Mechanical Properties of Reinforcement Steel

Table (4): Geometrical & Mechanical Properties of Carbon/Epoxy Composite Coupons

Table (5): Modes of Failure of Wall Specimens

Table (6): Ductility of Different Wall Specimens

Table (1): Shear Walls Test Matrix

Wall Specimen	Description	Application
C-S	Solid wall with no openings	Control
C-WO	Wall with a window opening of 2'x 2' at the center of the wall	Control
C-DO	Wall with a door opening of 1.5'x4' near the edge of the wall	Control
R-WO	Wall with a window opening of 2'x 2' at the center of the wall	Retrofitted
R-DO	Wall with a door opening of 1.5'x4' near the edge of the wall	Retrofitted

Table (2): Concrete Compressive Strength

Age	**Average Compressive Strength psi (MPa)**
28 days	3,705 (25.54)
on test date	6,550 (45.16)

Table (3): Mechanical Properties of Reinforcement Steel

Steel Rebar Size *mm [inches]*	**Average Yield Stress MPa [ksi]**	**Average Ultimate Strength MPa [ksi]**
9.5, 12.70 [0.375, 0.50]	468.84 [68]	620.53 [90]

Table (4): Geometrical & Mechanical Properties of Carbon/Epoxy (CFRP) Composite Coupons*

Laminate Description	**Ave. Width mm [inch]**	**Ave. Thickness mm [inch]**	**Ave. Ultimate Strength σ^{u}_{L}, MPa [ksi]**	**Ave. Modulus E_L, MPa [Msi]**	**Average Ultimate Strain**
Single-Ply Carbon/Epoxy Composite Laminate	24.23 [0.9538]	0.0407 (1.04)	992.5 [143.950]	62,121.76 [9.01]	1.6 %
2-Ply Carbon/Epoxy Composites	24.54 [0.966]	0.074 (1.88)	835.54 [121.184]	73,567.1 [10.67]	1.2 %

**ASTM D3039/D3039M*

Table (5): Modes of Failure of Wall Specimens

Wall Specimen	Description	Mode of failure
C-S	Solid wall with no openings	Flexure failure by concrete crushing at the wall toe
C-WO	Wall with a window opening of 2.00′ X 2.00′ at the center of the wall	Shear failure of the left and right piers at on the sides of the opening
C-DO	Wall with a door opening of 1.50′ X 4.00′ near the edge of the wall	Shear failure of the wide pier and flexure failure of the narrow pier on the sides of the opening
R-WO	Wall with a window opening of 2′ X 2′ at the center of the wall	Debonding of the CFRP laminates followed by flexure failure of the wall at zones between the piers and spandrels
R-DO	Wall with a door opening of 1.50′ X 4.00′ near the edge of the wall	Debonding of the CFRP laminates followed by flexure failure of the wall at zone between the narrow pier and top spandrel

Table (6): Ductility of Different Wall Specimens

Wall Specimen	**Yield Displacement (Δ_y), mm [inch]**	**Ultimate Displacement (Δ_c), mm [inch]**	$\mu_c = \frac{\Delta_c}{\Delta_y}$
C-S	6.3 [0.25]	31.8 [1.25]	5.00
C-WO	5.1 [0.20]	20.3 [0.80]	4.00
C-DO	5.1 [0.20]	24.10 [0.95]	4.75
R-WO	6.3 [0.25]	38.1 [1.50]	6.00
R-DO*	7.60 [0.30]	25.10 [1.00]	3.33

**Specimen failed prematurely due to severe debonding of CFRP laminates that caused splitting of the concrete cover*

List of Figures

Figure (1): Wall Specimens Details

Figure (2): Typical Test set-up

Figure (3): Cyclic Loading History in Accordance to ICC-ES AC 125-10

Figure (4): Typical Displacement Transducers Location for All Wall Specimens

Figure (5): Retrofit Schemes of Wall (R-WO) and Wall (R-WO)

Figure (6): Wall (R-DO) Anchorage System

Figure (7): Control Solid Wall (C-S) Failure

Figure (8): Load-Displacement Hysteresis Curves for Control Solid Wall (C-S)

Figure (9): Wall Specimen (C-WO) Failure

Figure (10): Load-Displacement Hysteresis Curves for Wall Specimen (C-WO)

Figure (11): Wall Specimen (C-DO) Failure

Figure (12): Load-Displacement Hysteresis Curves for Wall Specimen (C-DO)

Figure (13): Failure of Wall Specimen (R-WO)

Figure (14): Load-Displacement Hysteresis Curves for Wall Specimen (R-WO)

Figure (15): Failure of Wall Specimen (R-DO)

Figure (16): Load-Displacement Hysteresis Curves for Wall Specimen (R-DO)

Figure (17): Comparison of Load-Displacement Envelopes of All Wall Specimens

Figure (18): Comparison of Average Load Capacities of All Wall Specimens

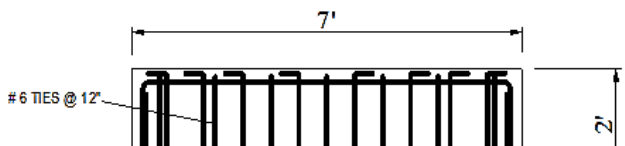

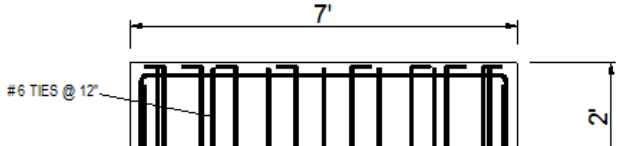

(a) Solid Wall Specimen (C-S)

(b) Wall Specimens with a Window Opening (C-WO) and (R-WO)

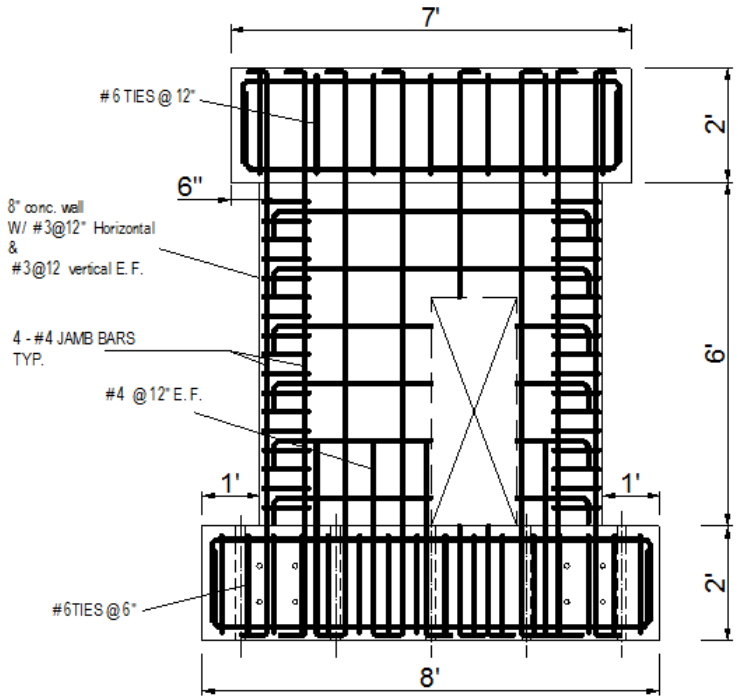

c) Wall Specimens with a Door Opening (C-DO) and (R-DO)

1 inch = 25.40 mm 1 foot =0.3048 m

Figure (1): Wall Specimens Details

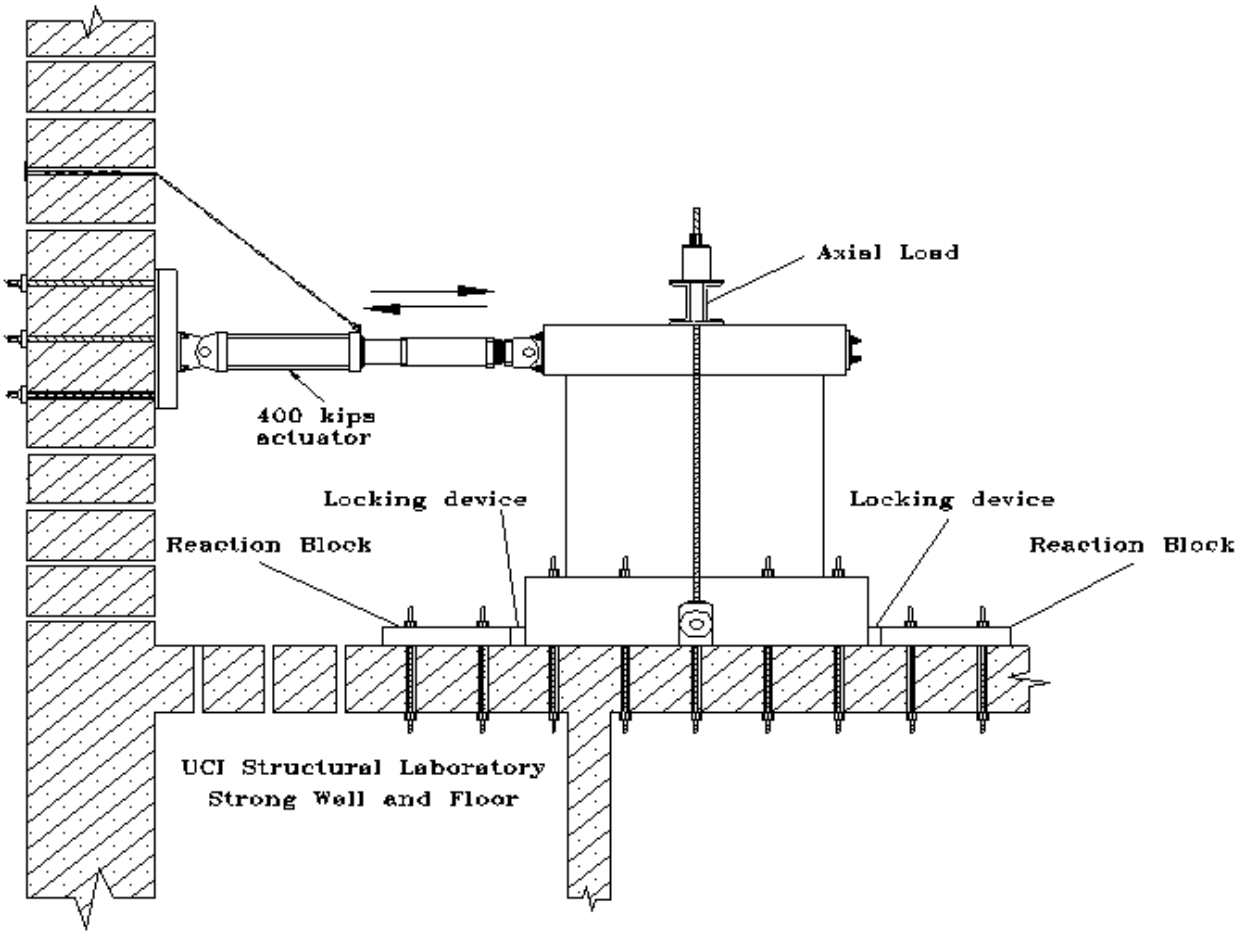

Figure (2): Typical Shear Walls Test Set-up

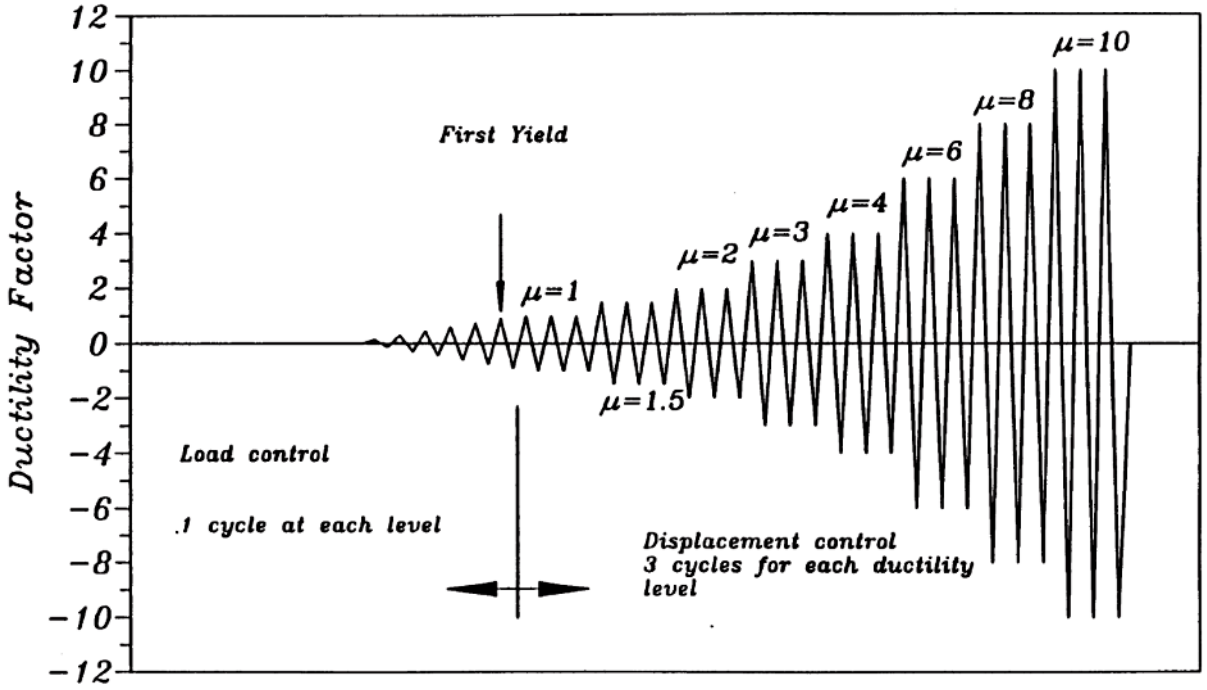

Figure (3): Cyclic Loading History in Accordance to ICC-ES AC 125-10

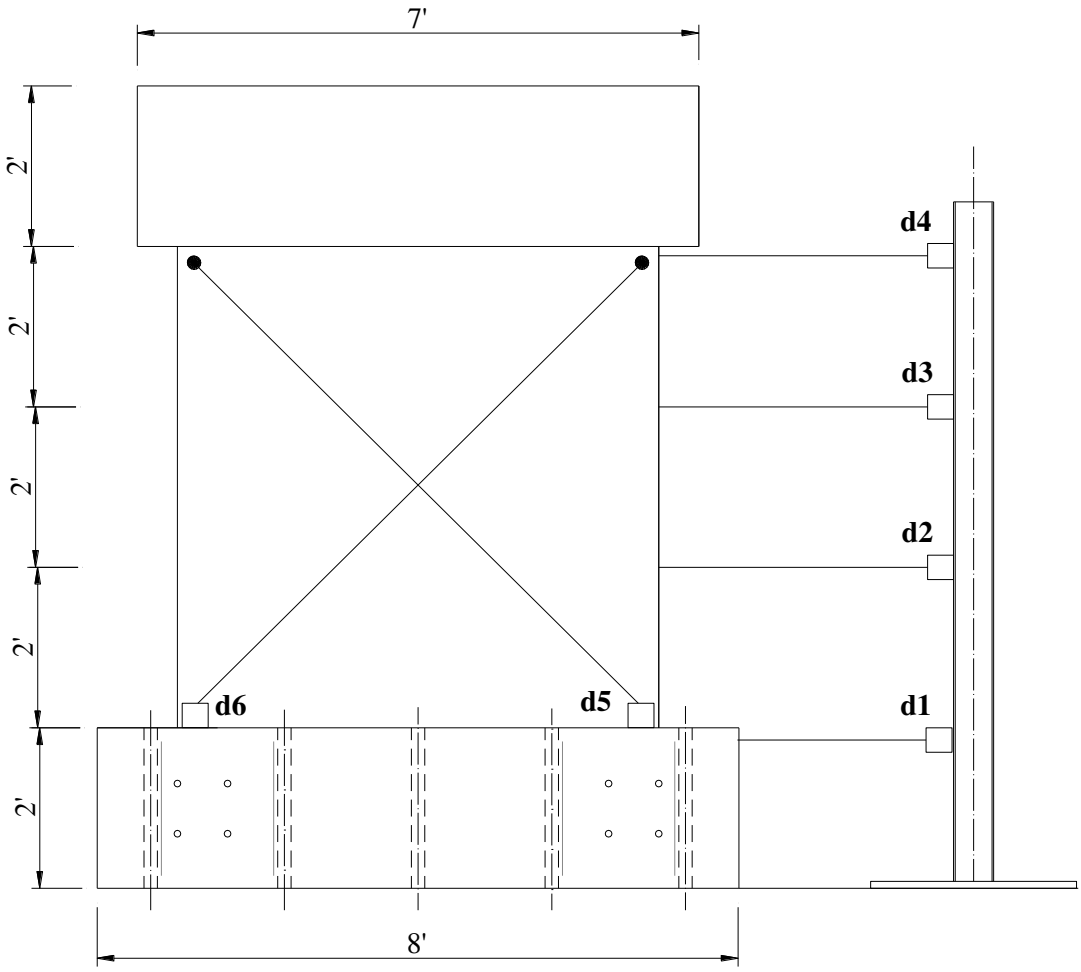

Figure (4): Locations of Displacement Transducers for All Wall Specimens

(a)

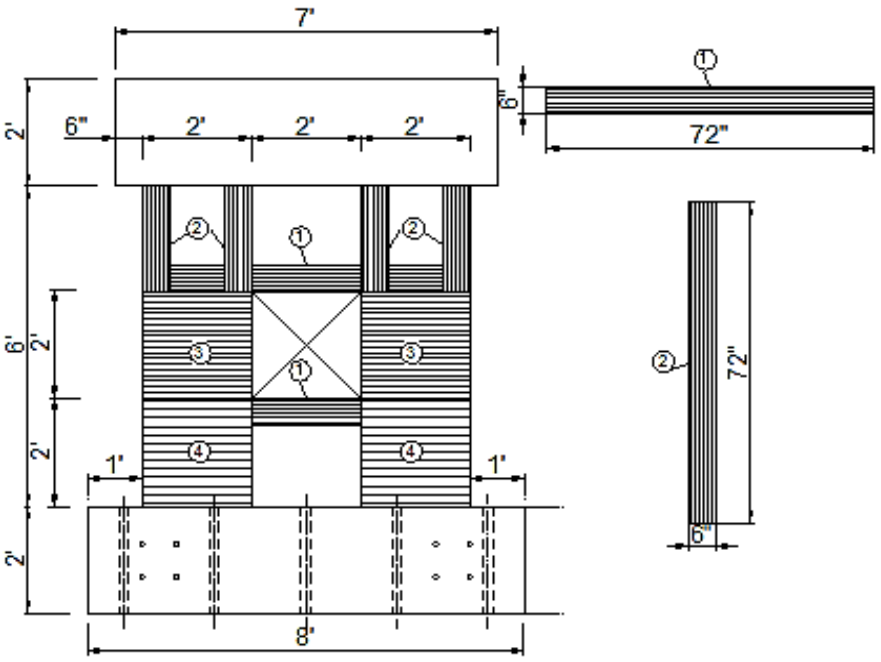

All Retrofit laminates 1 through 4 are 1 layer Carbon/Epoxy

Laminates 1 and 2 are applied on both sides of the wall , 3 is wrapped around and 4 is U-Shape.

(b)

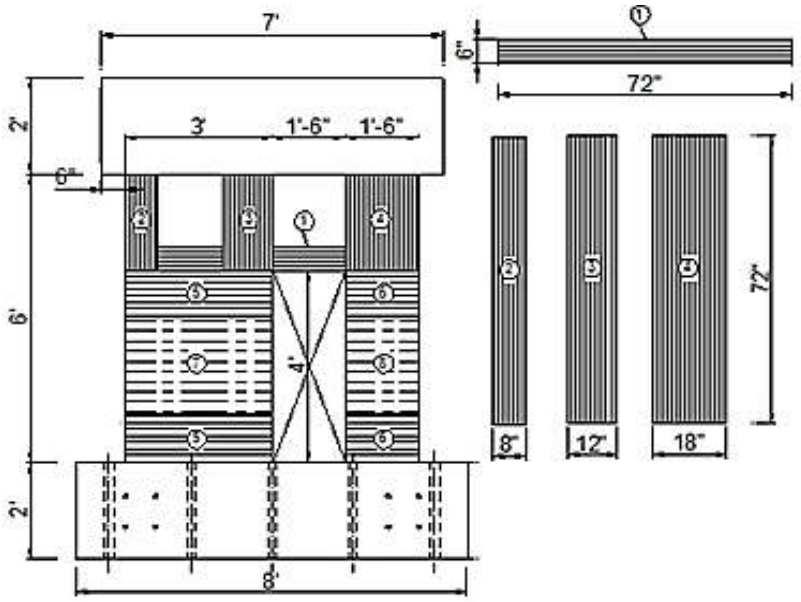

Retrofit laminates 1,5 and 6 are 1 layer Carbon/Epoxy FC061/RN075. Laminates 2, 3 and 4 are 2-layer Carbon/Epoxy

Laminates 1 through 4 are applied on both sides of the wall. Laminates 5 and 6 are wrapped around only for 12" at the top and bottom. Laminates 7 and 8 are U- Shape

Figure (5): Retrofit Schemes of: (a) Wall *R-WO*, and (b) Wall *R-DO*

Figure (6): Wall (R-DO) Anchorage System

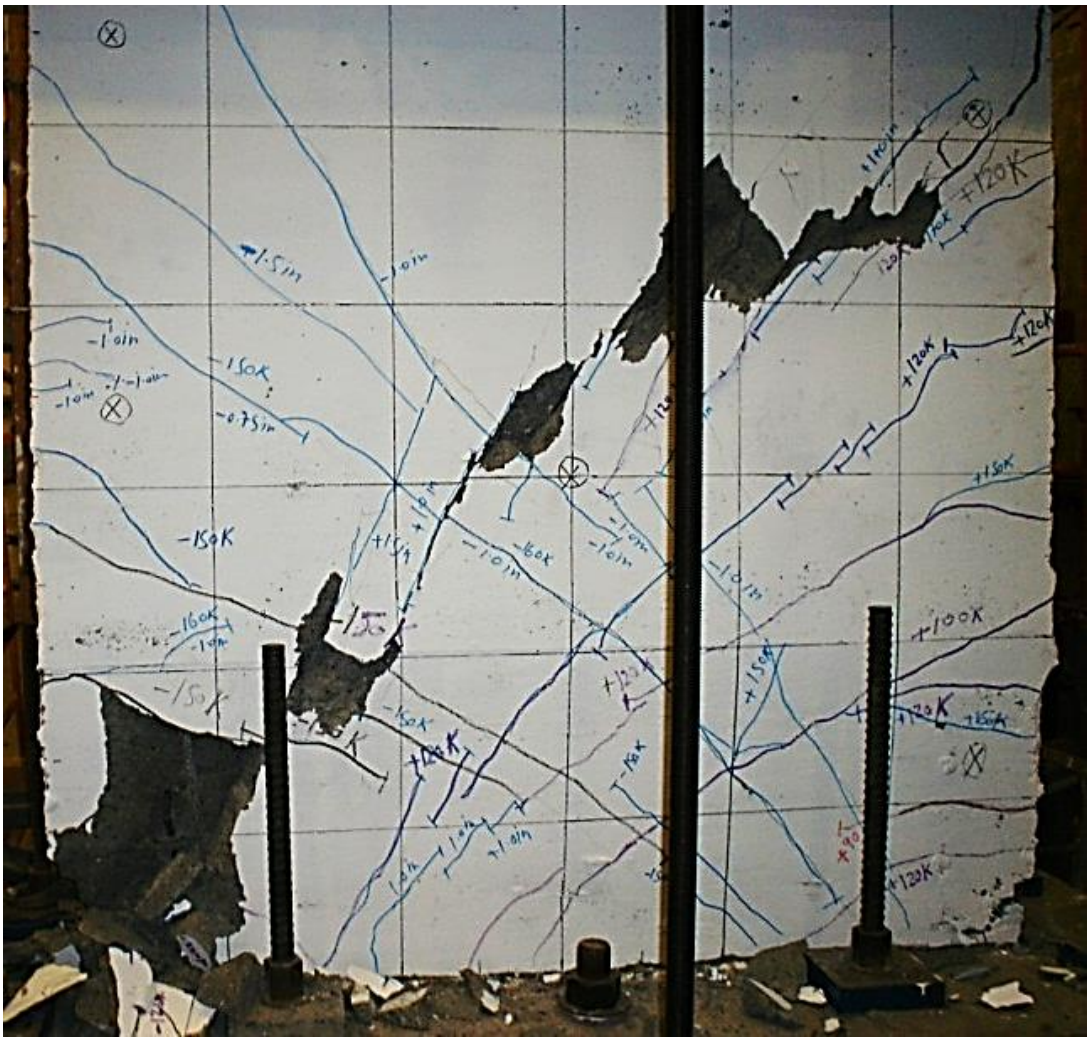

Figure (7): Control Solid Wall (C-S) Failure

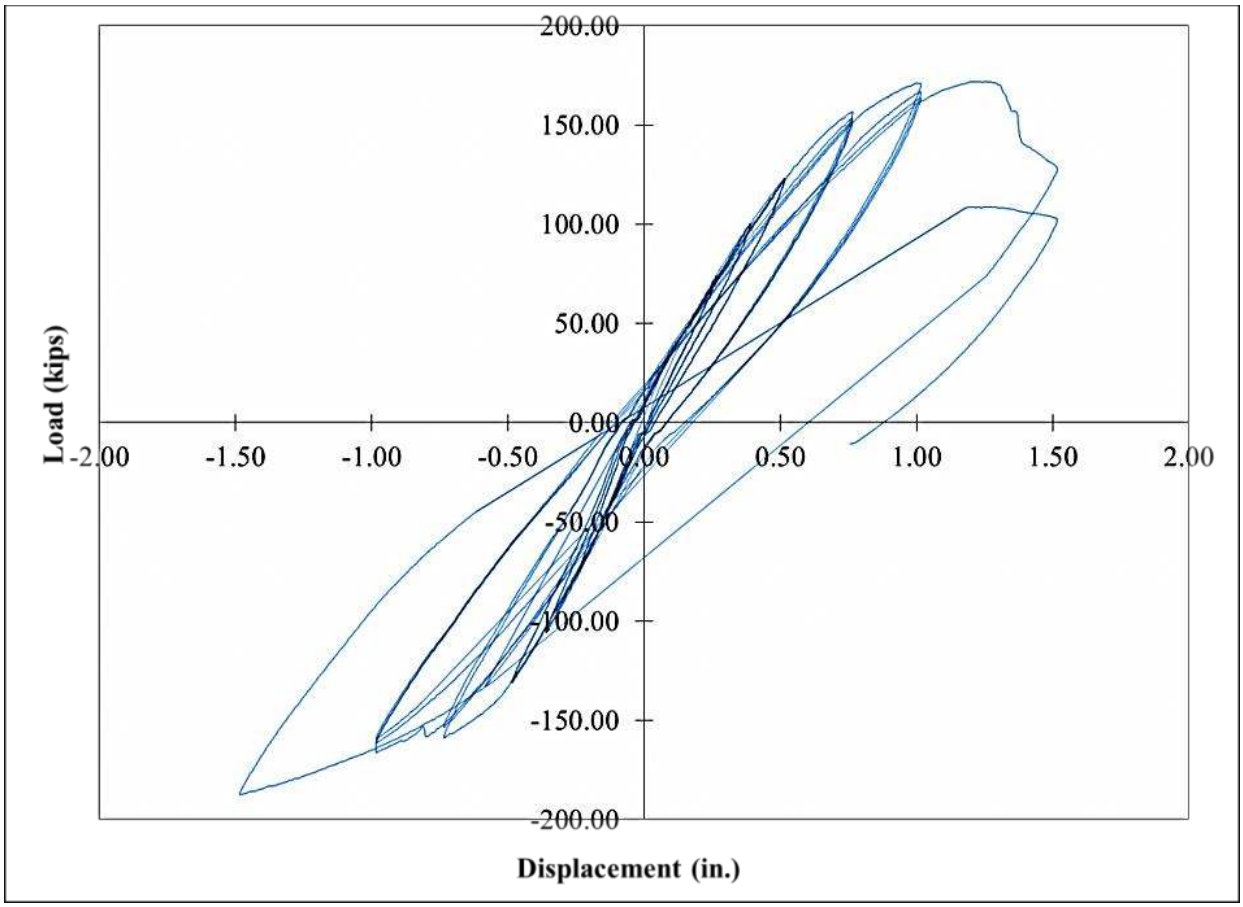

Figure (8): Load-Displacement Hysteresis Curves for Control Solid Wall (C-S)

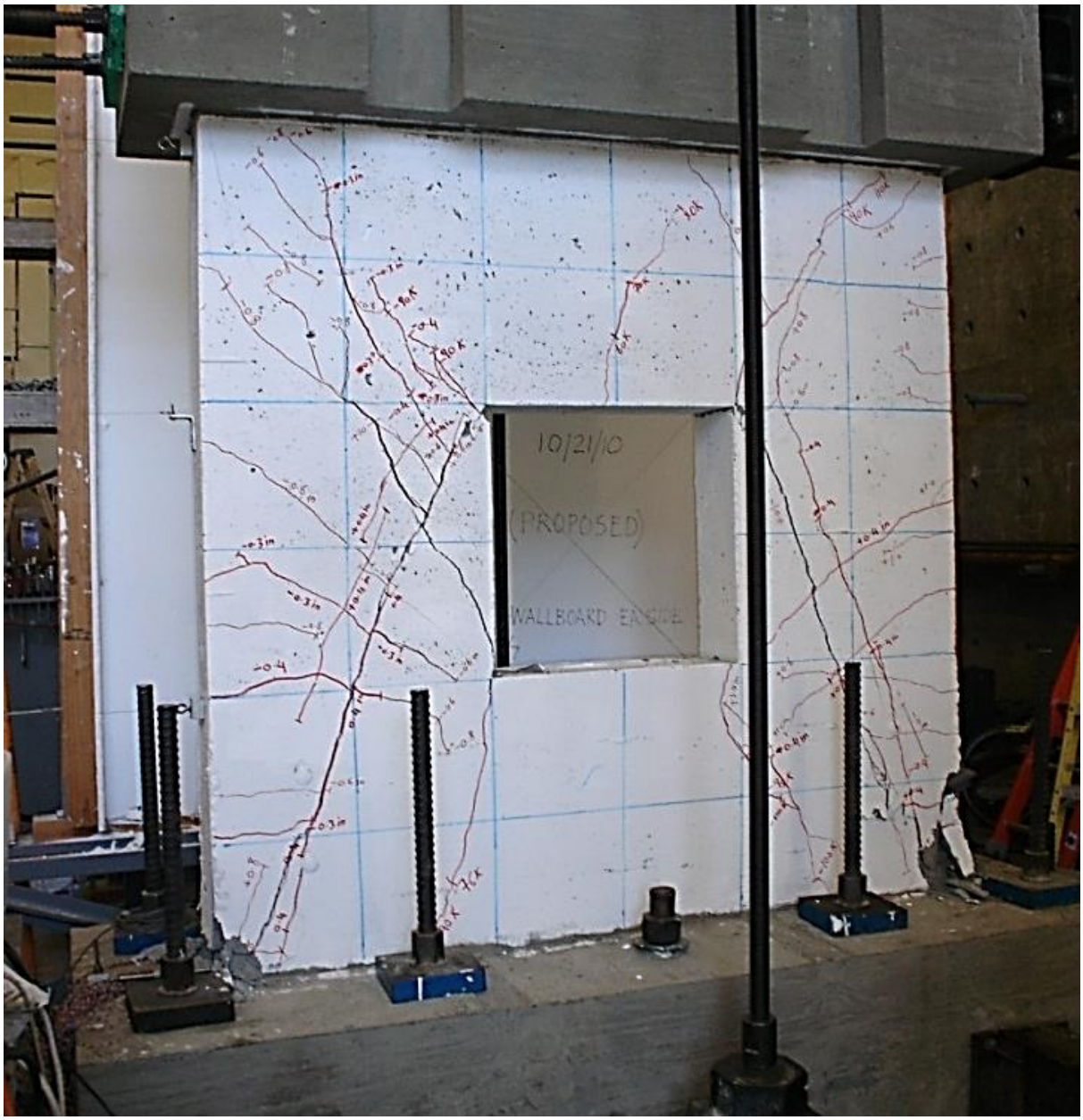

Figure (9): Wall Specimen (C-WO) Failure

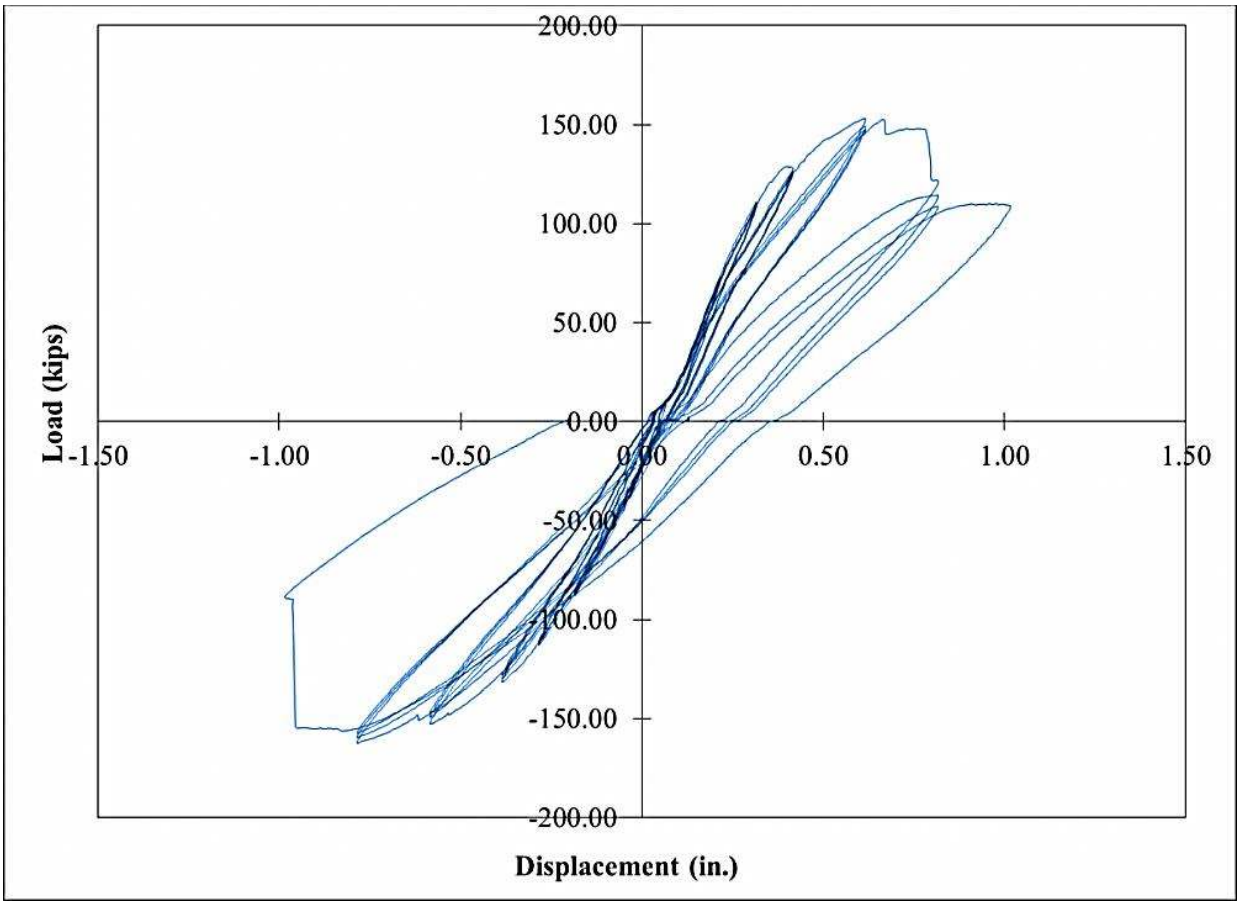

Figure (10): Load-Displacement Hysteresis Curves for Wall Specimen (C-WO)

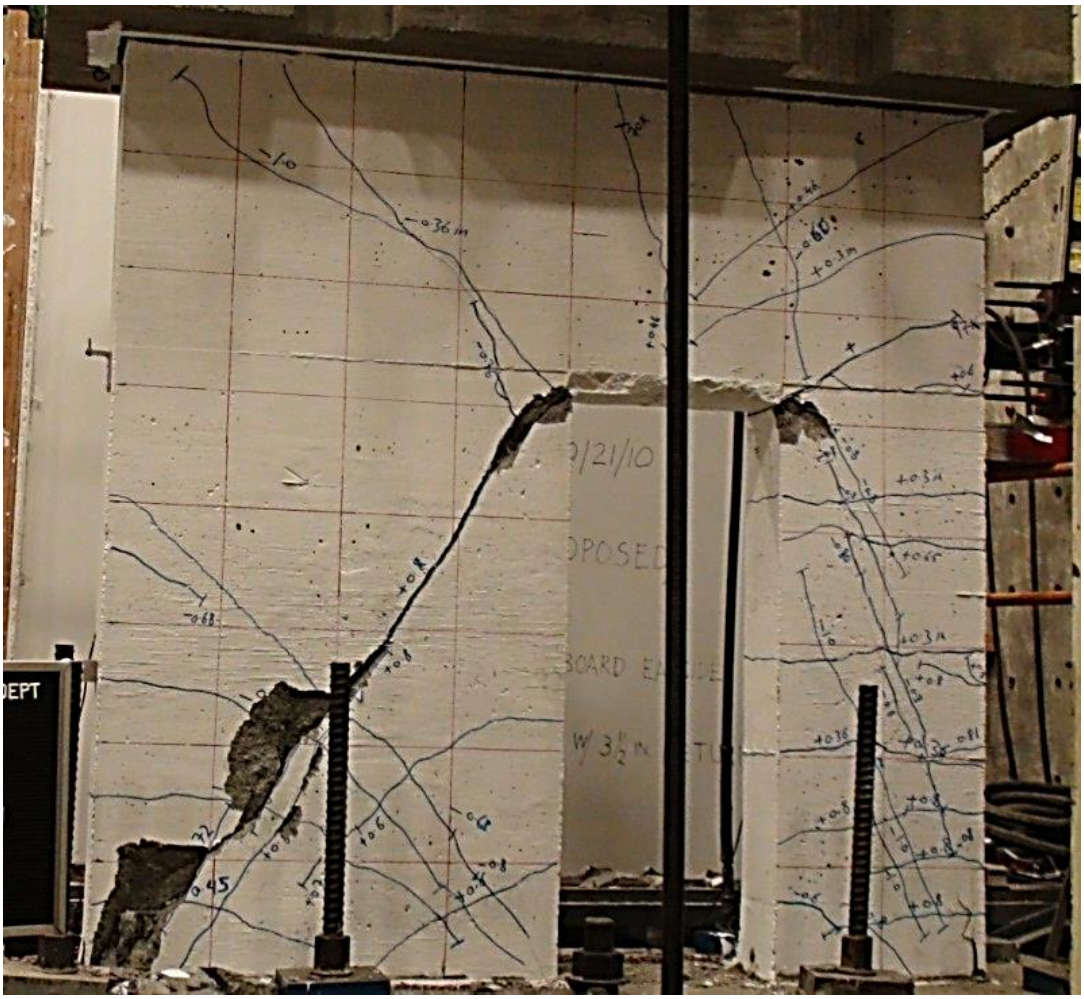

Figure (11): Wall Specimen (C-DO) Failure

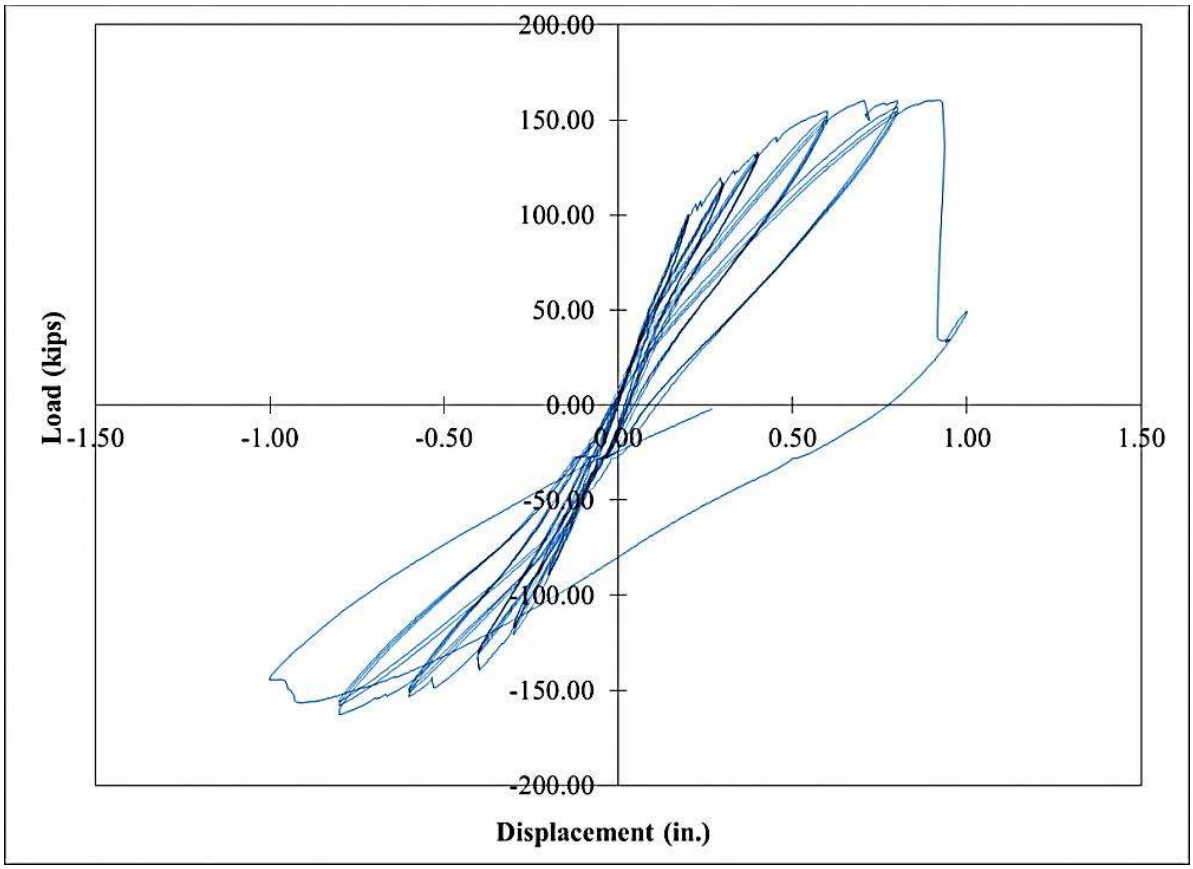

Figure (12): Load-Displacement Hysteresis Curves for Wall Specimen (C-DO)

Figure (13): Failure of Wall Specimen (R-WO)

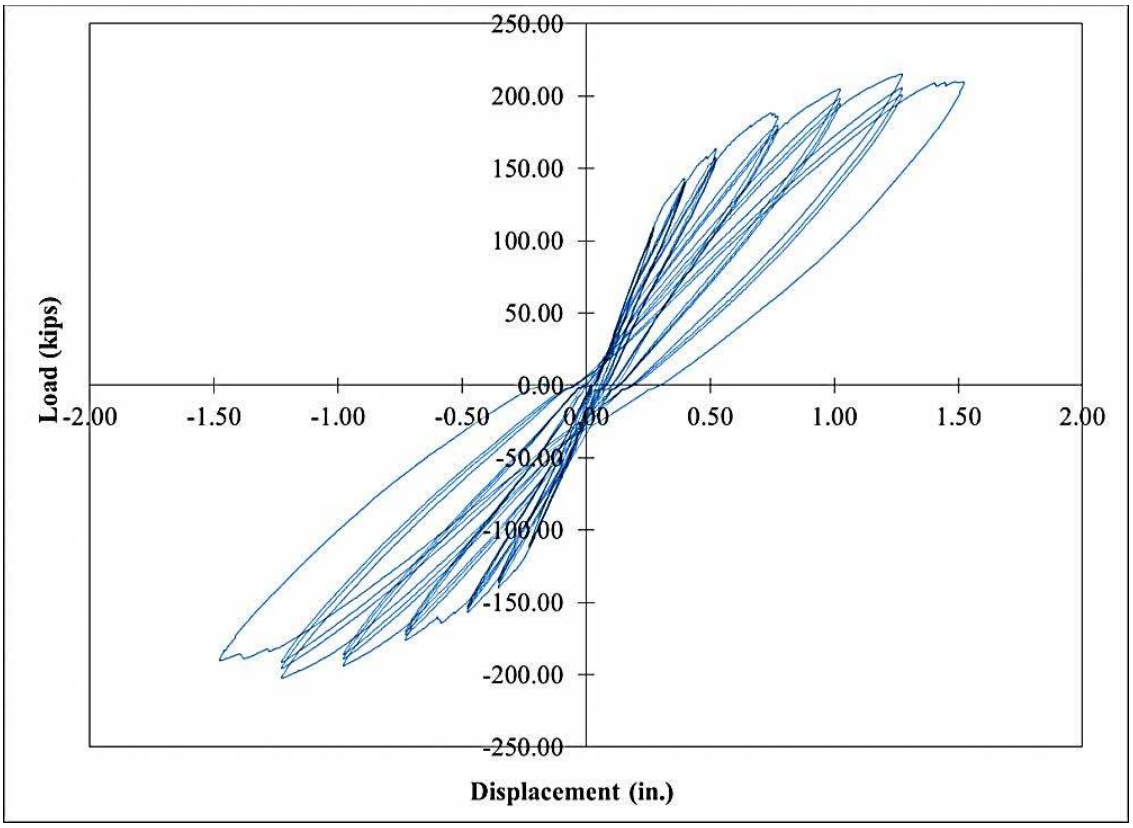

Figure (14): Load-Displacement Hysteresis Curves for Wall Specimen (R-WO)

Figure (15): Failure of Wall Specimen (R-DO)

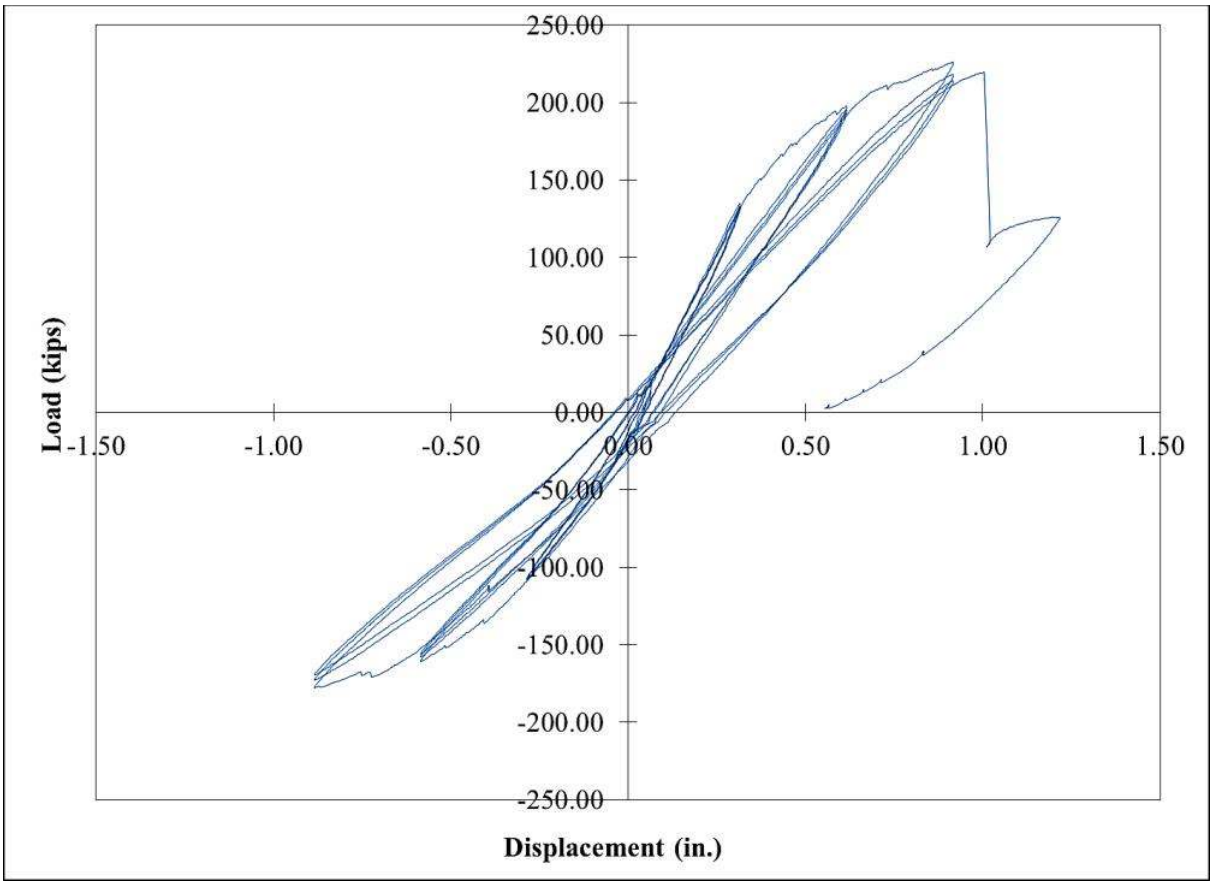

Figure (16): Load-Displacement Hysteresis Curves for Wall Specimen (R-DO)

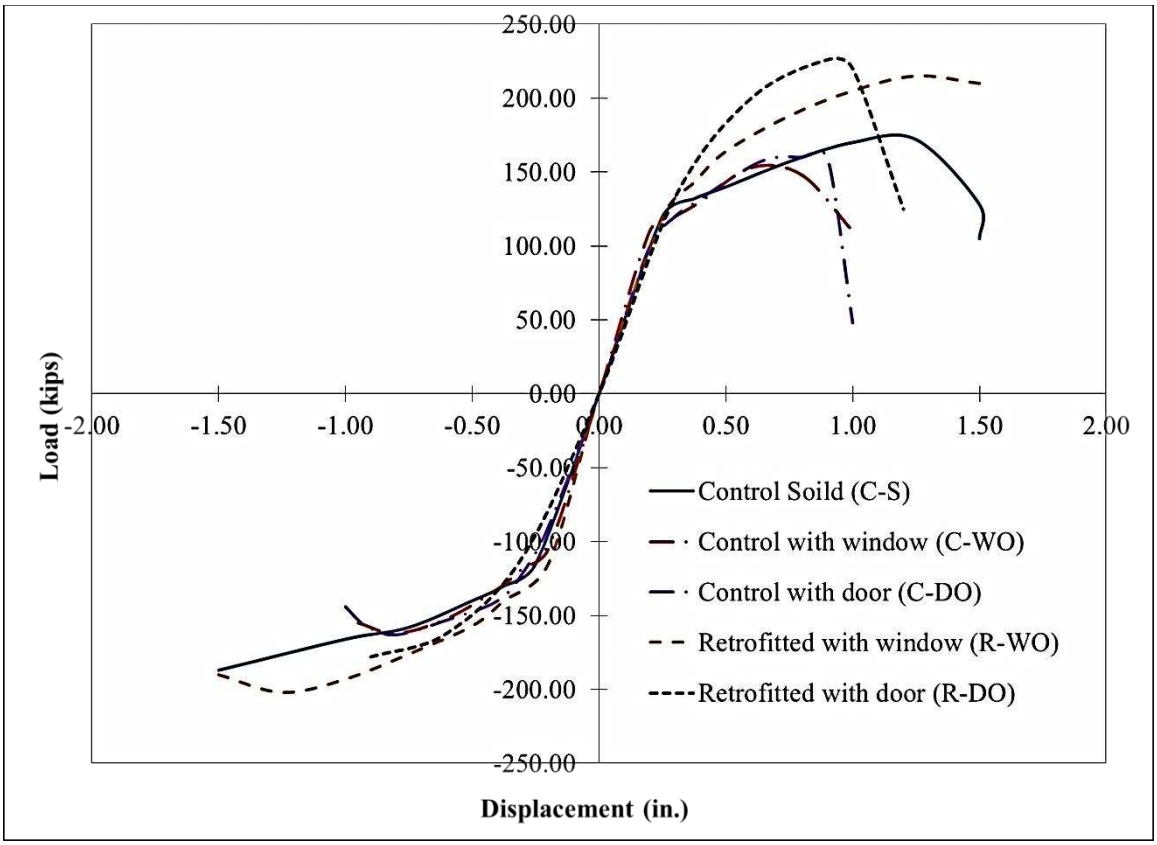

Figure (17): Comparison of Load-Displacement Envelopes of All Wall Specimens

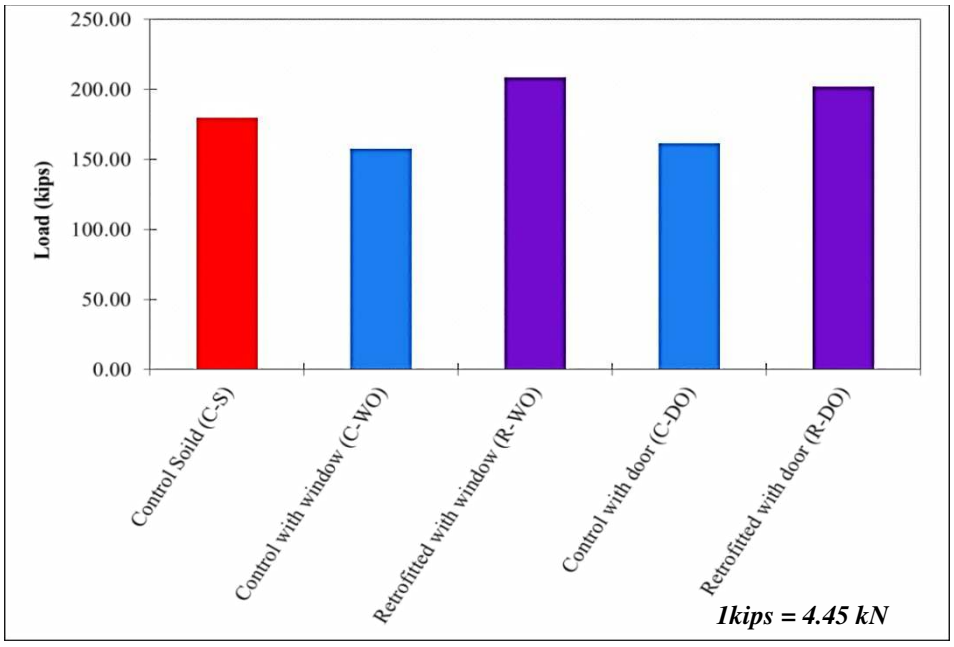

Figure (18): Comparison of Average Load Capacities of All Wall Specimens